J Bioenerg Biomembr (2010) 42:29–35
DOI 10.1007/s10863-009-9263-1

Coupling factor B affects the morphology of mitochondria

Grigory I. Belogrudov

Received: 16 September 2009 / Accepted: 20 October 2009 / Published online: 13 January 2010

Abstract Ectopic expression of coupling factor B in animal cells resulted in altered mitochondrial morphology. Cells expressing factor B fused to green fluorescent protein (GFP) contained fragmented, balloon-shaped or thinned, filamentous mitochondria, terminating at one end with balloon-like structures. Ultrastructural analysis using transmission electron microscopy revealed changes in the organization of mitochondrial cristae in cells expressing factor B-GFP fusion protein.

Keywords Coupling factor B · Inner mitochondrial membrane · Mitochondrial crista · Mitochondrial morphology

Introduction

To maintain viability and meet energy demands, living organisms use elaborate networks of biochemical pathways to extract efficiently energy stored in foodstuffs. The extracted energy is conserved in the form of ATP, most of which is synthesized during the oxidation of nutrient-derived metabolites in the course of oxidative phosphorylation that occurs in mitochondria. The extensive infoldings of the inner mitochondrial membrane, called cristae, are highly enriched with membrane-bound enzyme complexes that constitute the oxidative phosphorylation system (Hatefi 1985). The function of the inner membrane as a permeability barrier to ions, including protons, and cellular metabolites, is essential for maintenance of an electrochemical proton gradient at values sufficiently high to drive the synthesis of ATP.

In the mitochondria of animal cells, coupling factor B facilitates the energy-driven synthesis of ATP catalyzed by the mitochondrial ATP synthase complex (Belogrudov 2002; Belogrudov 2009; Belogrudov and Hatefi 2002; Lam et al. 1967; Sanadi 1982). Previous studies have demonstrated that depletion of factor B from ammonia / EDTA-treated bovine heart submitochondrial particles (AE-SMP) abolishes oxidative phosphorylation and its partial reactions (Belogrudov 2002; Belogrudov and Hatefi 2002; Lam et al. 1967; Sanadi 1982). Early experiments of Lee and Ernster (1965) demonstrated the restoration of energy-driven reactions in AE-SMP treated with the antibiotic oligomycin, a specific inhibitor of proton translocation through membrane sector F_O of the eukaryotic ATP synthase (Hong and Pedersen 2008). The effect of oligomycin provided the first evidence that uncoupled from ATP synthesis backflow of protons through sector F_O might constitute a mechanism by which protons leak through the membranes of AE-SMP. More recently, we have demonstrated that recombinant human, or bovine, factor B polypeptides repair more efficiently than oligomycin proton leak associated with AE-SMP (Belogrudov 2002, 2006, 2008; Belogrudov and Hatefi 2002).

Recent advances in structure-functional studies of factor B have provided valuable insights into its role in the mechanism of oxidative phosphorylation in the mitochondria of animal cells (Belogrudov 2009). The proximity of bovine factor B to F_O subunits *e* and *g*, as well as to the ADP/ATP carrier, was established in cross-linking experiments using a factor B mutant containing a photo-reactive, unnatural amino acid substituted for the Trp2 residue (Belogrudov 2008). Our earlier cross-linking studies had

G. I. Belogrudov (✉)
West Los Angeles Veterans Administration Medical Center,
11301 Wilshire Blvd.,
Los Angeles, CA 90073, USA
e-mail: gbelo@ucla.edu

demonstrated the proximity between subunits *e*, *f*, and *g* (Belogrudov et al. 1996), between subunits *f* and *A6L* (Belogrudov et al. 1996), and between *A6L* and subunit *d* (Belogrudov et al. 1995). Additional structure-functional studies demonstrated the importance of the N-terminal residues of factor B, showing that deletion of amino acid sequence Trp2-Gly3-Trp4 resulted in a decrease in both the coupling activity and the ability of a factor B mutant to block passive proton diffusion by F_O-reconstituted proteoliposomes (Belogrudov 2008). Finally, the crystal structure of bovine factor B determined at 0.96 Å resolution demonstrated that the first ten amino acids of the polypeptide, including Trp2, form a short α helix, which extends away from the molecule's body (Lee et al. 2008). Based on these structure-functional analyses, we have proposed that membrane sector F_O of the ATP synthase complex is comprised of two proton translocation pathways and that the proton translocation activity of one of the pathways is regulated via interaction with the N-terminal α helix of factor B (Belogrudov 2009; Belogrudov and Hatefi 2002; Lee et al. 2008).

Of the two proton translocation pathways, one pathway encompasses a ring of the oligomeric subunit *c* and two half-channels located at the interface between the F_O *a* subunit and the subunit *c* ring (Fillingame et al. 2003; Junge et al. 2009; Vik et al. 2000). The other pathway is predicted to be formed from the transmembrane segments of the F_O subunits *e*, *f*, *g*, *A6L*, and, possibly, segments provided by the ADP/ATP carrier (Belogrudov 2009). Occlusion of the latter pathway by the N-terminal α helix of factor B inhibits its proton-translocation activity, while the former pathway, which involves the subunit *c* rotory motor, carries out proton transport when respiration is coupled to ATP synthesis. Extraction of factor B from AE-SMP relieves blockade by the N-terminal α helix, allowing uncoupled from ATP synthesis proton translocation and dissipation of a transmembrane proton gradient. Thus, the interaction of factor B with membrane sector F_O is important not only for the protein's coupling activity, but also for regulation of the electrochemical proton gradient across the inner mitochondrial membrane. The existence of two proton "channels" within the membrane sector F_O was also suggested based on analysis of inhibition by dicyclohexylcarbodiimide of active and passive proton translocation in bovine submitochondrial particles (Kopecky et al. 1981).

Recently, we reported that the 24-amino acid long sequence located upstream of the N-terminal phenylalanine of the mature human factor B represents a mitochondria-targeting leader, which localizes the polypeptide to mitochondria in HEK293 cells (Belogrudov 2007). In the course of subsequent studies, we ectopically expressed human factor B as a fusion protein with GFP in a number of animal cell lines and performed their characterization using confocal and transmission electron microscopy. Here we present experimental evidence demonstrating that ectopic expression of coupling factor B affects the morphology of mitochondria.

Materials and methods

Plasmid construction

Plasmids, pAcGFP1-N1-Δ1-15FB and pGB-GFP, were previously described (Belogrudov 2007). Plasmid pAcGFP1-N1-Δ1-15FB contains a cDNA sequence encoding a full-length mature human factor B sequence with its endogenous 24-amino acid long mitochondria-targeting leader cloned 5' to a cDNA sequence encoding a monomeric GFP in the pAcGFP1-N1 plasmid (Clontech). Plasmid pGB-GFP contains a 24-amino acid long human factor B mitochondria-targeting leader cloned 5' to a cDNA sequence encoding a monomeric GFP in the pAcGFP1-N1 plasmid. The mitochondrial localization of fusion proteins FB-GFP and mito-GFP encoded by these plasmids was previously demonstrated (Belogrudov 2007).

Cell culture, transfection, and selection of stable cell lines

Human embryonic kidney cells, HEK293, human cervix adenocarcinoma epithelial cells, HeLa, and pig kidney proximal tubule epithelial cells, LLC-PK_1, were purchased from ATCC. Embryonic mouse cardiomyocyte cells, HL-1, were generously provided by Dr. William C. Claycomb (Louisiana State University Health Sciences Center, New Orleans, LA). HEK293, HeLa, and LLC-PK_1 cells were maintained in DMEM containing 4.5 g/l glucose, 0.11 g/l sodium pyruvate, 2 mM L-glutamine, 10% fetal bovine serum (FBS), 100 U/ml penicillin, and 100 μg/ml streptomycin in a humidified atmosphere with 5% CO_2 at 37°C. HL-1 cells were maintained in Claycomb medium containing 2 mM L-glutamine, 0.1 mM norepinephrine, 10% FBS (SAFC Biosciences), 100 U/ml penicillin, and 100 μg/ml streptomycin in a humidified atmosphere with 5% CO_2 at 37°C. Upon reaching confluency, some groups of HL-1 cells have demonstrated the contractile activity.

Cells were transfected with plasmid constructs using Optifect transfection reagent (Invitrogen) according to the manufacturer's recommendations. Selection of stably transfected LLC-PK_1 cells was performed by seeding transfected cells at a low density on 100 mm round dishes in DMEM, which in addition to the previously specified supplements also included 1.5 mg/ml G418. GFP-expressing clones were isolated, expanded, and subjected to an additional round of selection in the presence of G418. Stably transfected clones of LLC-PK_1 cells were maintained in the presence of 0.3 mg/ml G418.

Confocal microscopy of living cells

Cells were seeded on collagen- or gelatin / fibronectin-coated MatTek glass bottom dishes (MatTek Corp.) and transfected as described above. Living cells were imaged using a confocal microscope 24–36 h post-transfection. Stably transfected LLC-PK_1 cells were allowed to adhere for at least 24 h before confocal microscopy analysis. To qualitatively assess mitochondrial membrane potential (Fig. 2a), cells were incubated with 20 nM $DiIC_1(5)$ (Invitrogen) for 30 min prior to imaging. To label the ER network (Fig. 2b), LLC-PK_1 cells stably expressing factor B-GFP fusion protein were transfected with DsRed2-ER plasmid (Clontech), which encodes an endoplasmic reticulum targeting sequence derived from calreticulin fused to the 5' end of a human codon-optimized DsRed2 fluorescent protein, followed by the ER retention sequence, KDEL. Living cells were imaged 36 h post-transfection.

Images were acquired using a confocal microscope LSM 510 (Carl Zeiss AG) with attached Axiovert 100 M fluorescence microscope. A plan-Apochromat 100x/1.4 NA oil iris objective lens was used. Images presented in Fig. 1 were acquired using a single-track configuration (argon laser 488 nm excitation, LP 505 nm emission filter). Collected serial images (z-stacks) were processed into three-dimensional projections using LSM 510 software, version 3.2. Images shown in Fig. 2a were acquired using a single-track configuration (argon laser 488 nm excitation, BP 505–530 nm emission filter/HeNe2 laser 633 nm excitation, LP 650 nm emission filter). Images shown in Fig. 2b were acquired using a multi-track configuration (argon laser 488 nm excitation, BP 505–530 nm emission filter/HeNe1 laser 543 nm excitation, LP 560 nm emission filter).

Transmission electron microscopy

LLC-PK_1 cells stably expressing either FB-GFP or mitochondria-targeted GFP were grown in T25 plastic flasks. Cells were fixed in 2% glutaraldehyde, 2% formaldehyde in 0.1 M sodium cacodylate buffer, pH 7.4, and washed with the same buffer. After a post-fixation in 1% OsO_4, the cells were dehydrated in a graded series of

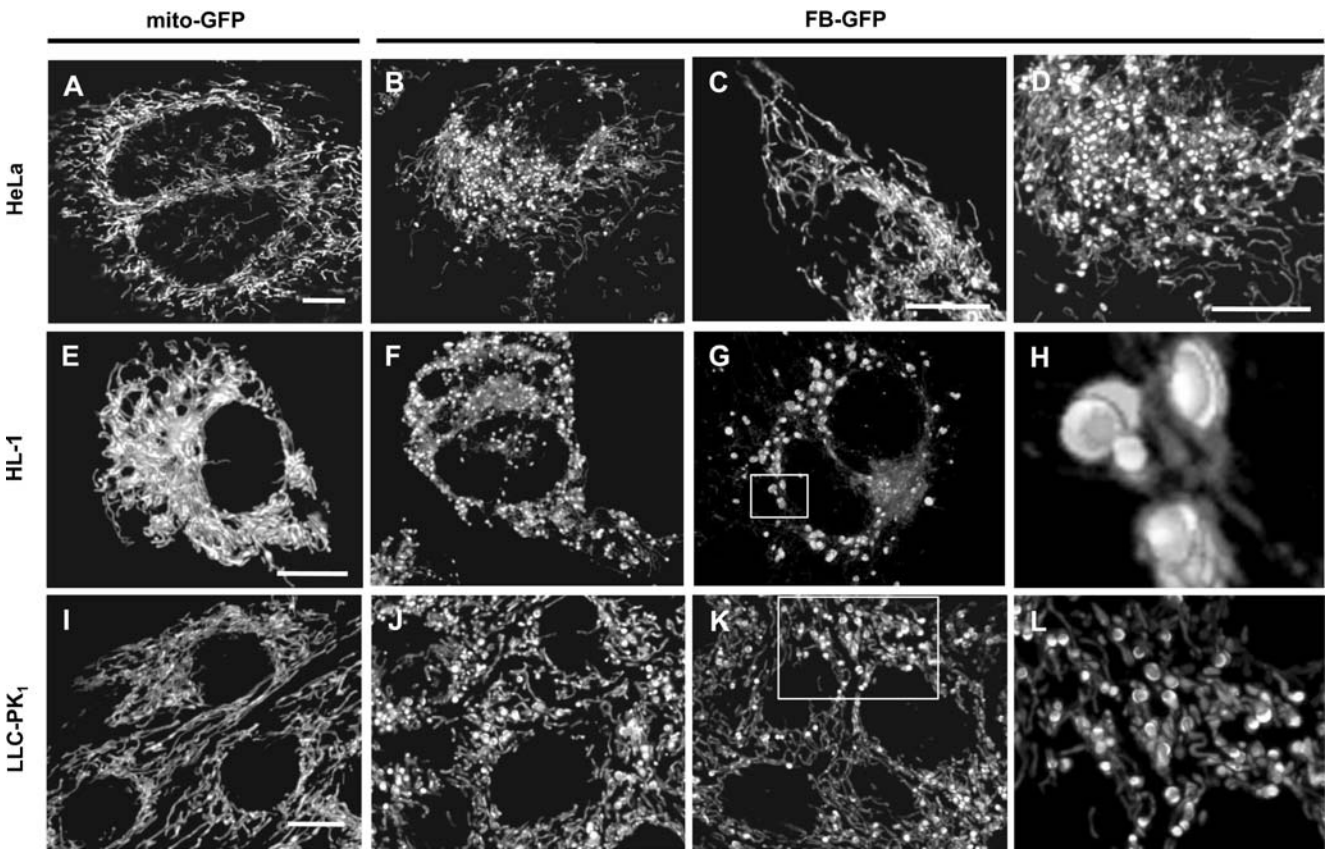

Fig. 1 Confocal microscopy of living cells transiently or stably expressing mito-GFP or FB-GFP fusion protein. HeLa and HL-1 cells transiently expressing mito-GFP (**a**, **e**) or FB-GFP fusion protein (**b-d**, **f-h**) are shown. LLC-PK_1 cells stably expressing mito-GFP or FB-GFP fusion protein are shown in panels I and J-L, respectively. The boxed areas in G and K were magnified and are shown in panels H and L, respectively. Bars, 10 μm

ethanol, treated with propylene oxide, and embedded in Eponate 12 (Ted Pella, Inc.). Sections (60–70 nm) were cut on a Reichert-Jung Ultracut E Ultramicrotome and picked up on formvar coated copper grids. Sections were stained with uranyl acetate and Reynolds lead citrate and examined on a JEOL 100CX electron microscope at 80 kV. Electron microscopy specimens were prepared by Marianne Cilluffo (UCLA Brain Research Institute), and were subsequently analyzed by G.I.B.

Results

Figure 1 shows confocal microscopy images of living cells transiently (Fig. 1**a**-**h**) or stably (Fig. 1**i**-**l**) expressing mito-GFP (Fig. 1**a**, **e**, **i**) or FB-GFP (Fig. 1**b**-**d**, **f**-**h**, **j**-**l**) proteins. Transient expression of FB-GFP fusion protein in HeLa, HL-1, and HEK293 (not shown) cells resulted mostly in fragmented, balloon-shaped mitochondria (Fig. 1**b**-**d**, **f**, **g**). LLC-PK_1 cells stably expressing FB-GFP fusion protein contained thinned, filamentous mitochondria, terminating at one end with balloon-like structures (Fig. 1**j**, **k**). Higher magnification (Fig. 1**h**, **l**) revealed disk-shaped structures, apparently attached to one another. These are proposed to be mitochondria undergoing division.

To qualitatively assess mitochondrial membrane potential, LLC-PK_1 cells stably expressing FB-GFP fusion protein were stained with the fluorescent dye $DiIC_1(5)$, which is taken up by mitochondria in a membrane potential-dependent manner (Fig. 2**a**). In the merged image of Fig. 2**a**, the mitochondria with balloon-like structures strongly stained with the dye, indicating the existence of high membrane potential across their inner membranes.

Next, LLC-PK_1 cells stably expressing FB-GFP fusion protein were transfected with a plasmid encoding a fluorescent marker that localizes to the endoplasmic reticulum. The merged image of a transfected cell shown in Fig. 2b reveals no significant overlap between green and red fluorescence, confirming the exclusive localization of coupling factor B to mitochondria.

Finally, the ultrastructure of mitochondria in LLC-PK_1 stable cell lines was investigated using transmission electron microscopy (Fig. 3). Mitochondria with normally developed cristae were observed in LLC-PK_1 cells express-

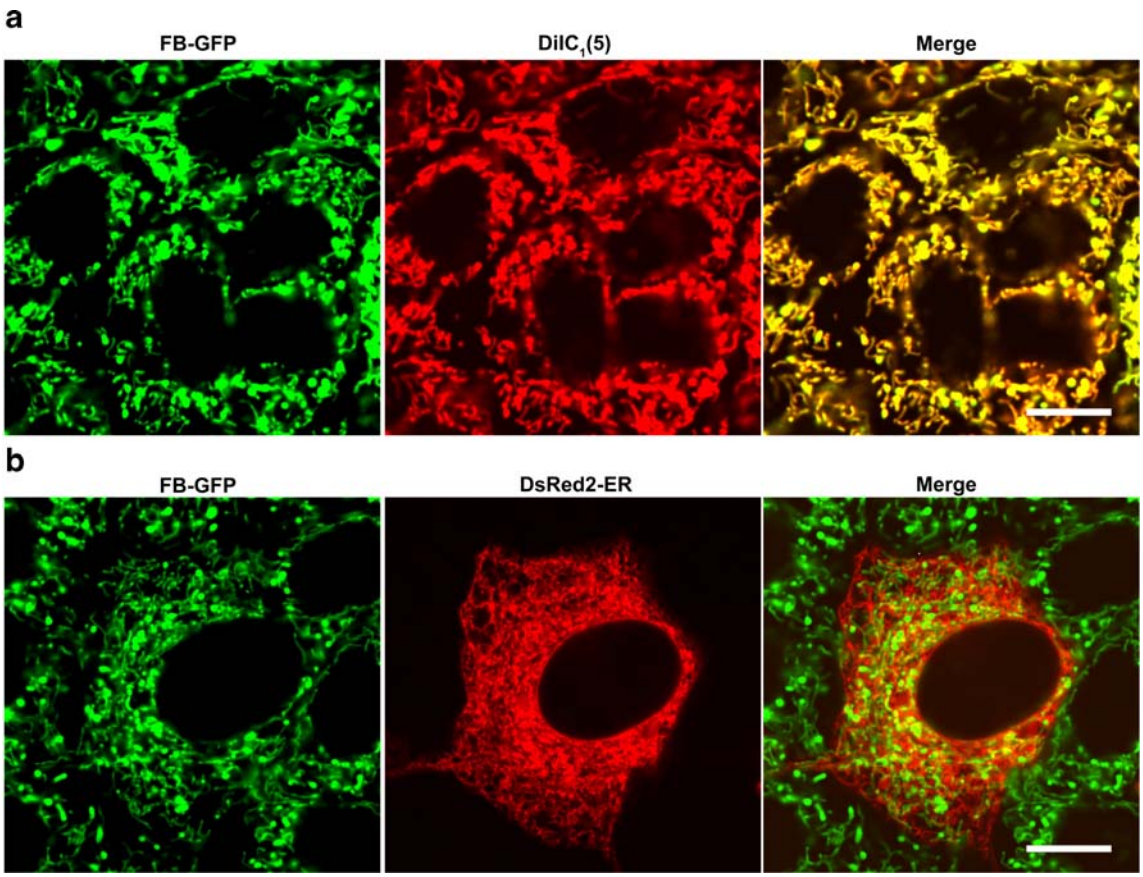

Fig. 2 Confocal microscopy of living LLC-PK_1 cells stably expressing FB-GFP fusion protein. **a** Cells were imaged following incubation with a mitochondrial membrane potential-sensitive dye $DiIC_1(5)$. **b** A cell transiently transfected with DsRed2-ER plasmid, encoding a red fluorescent protein targeted to the endoplasmic reticulum, is shown. Bars, 10 μm

ing mito-GFP (Fig. 3a). In contrast, in cells expressing FB-GFP fusion protein mitochondria displayed either elongated cristae that localized along the organelle's perimeter or cristae that formed half-rings (Fig. 3b-f).

Discussion

Numerous cell biology studies have provided convincing evidence regarding the remarkable plasticity in the shape and connectivity displayed by mitochondria in cultured animal cells (Beraud et al. 2009; Collins et al. 2002; Wasilewski and Scorrano 2009). Processes involving the turnover of mitochondrial protein and lipid components, degradation via mitophagy, as well as fission and fusion, all contribute to mitochondrial homeostasis in a living cell. The mitochondrial fusion and fission machinery comprises proteins that reside within mitochondrial membranes, translocate to the mitochondria from the cytoplasm, or localize to both the mitochondria and the endoplasmic reticulum (Berman et al. 2009; Chan 2006; de Brito and Scorrano 2008; Pauleau et al. 2008; Wasilewski and Scorrano 2009). In spite of numerous reports on mitochondrial dynamics in various cell types, uncertainty remains as to whether morphological alterations impinge on the organelle's bioenergetic capacity (Benard and Rossignol 2008).

Here we present experimental evidence that ectopic expression of coupling factor B alters the morphology of mitochondria in cultured animal cells. Morphological changes were readily observed at the whole organelle and ultrastructural levels in cells expressing human factor B-GFP fusion protein either transiently or stably. A monomeric GFP was used to visualize the subcellular localization of ectopically expressed proteins. Based on assays of factor B coupling activity (Belogrudov 2002; Belogrudov and Hatefi 2002; Lam et al. 1967; Sanadi 1982; Stephenson and Sanadi 1989), the protein is predicted to bind to the matrix side of the inner mitochondrial membrane, suggesting that in cultured cells the human factor B mitochondrial leader delivers both GFP and FB-GFP to the mitochondrial matrix. Previous studies have demonstrated the ability of factor B to block proton leak in AE-SMP (Belogrudov 2002; Belogrudov and Hatefi 2002; Sanadi 1982) and inhibit passive proton diffusion of F_O-reconstituted proteoliposomes (Belogrudov 2008). Considering these results, we propose that changes in mitochondrial morphology described here could be linked to hyperpolarization of the inner membrane, caused by an increase in the level of membrane-bound factor B.

Yeast strains with genetically modulated expression levels of ATP synthase subunits *e* or *g* contain mitochondria whose cristae are organized in onion-like structures (Arselin

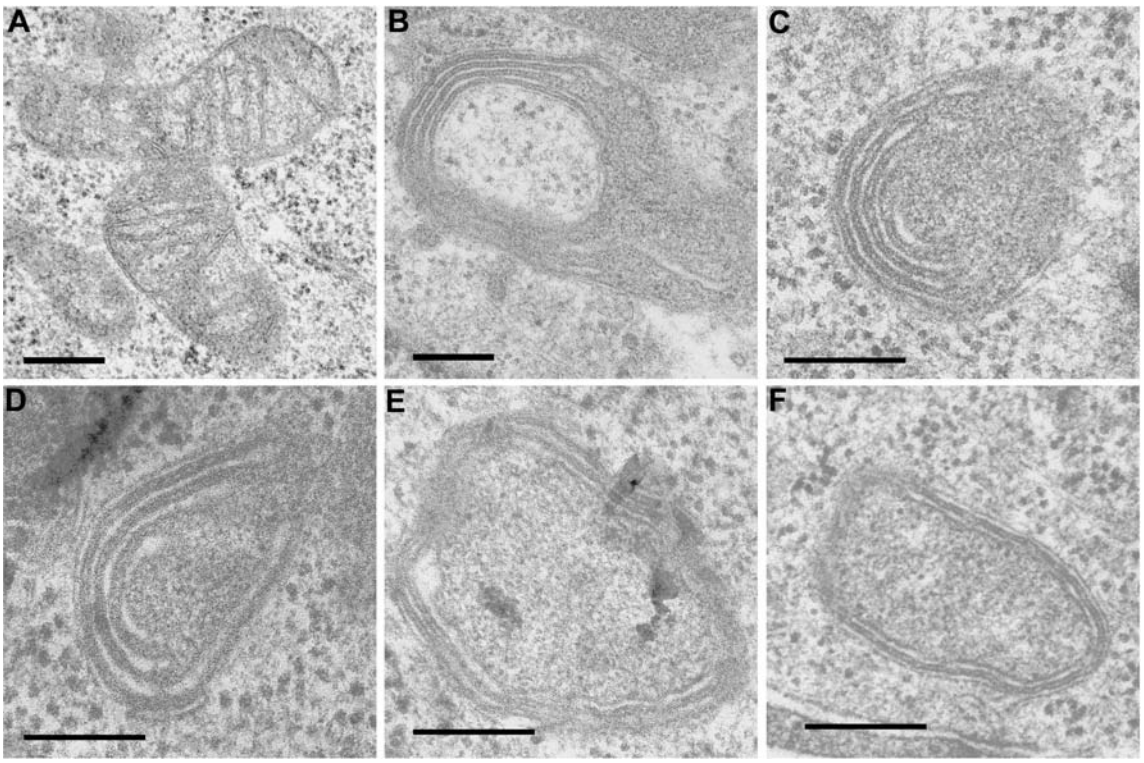

Fig. 3 Ultrastructural analysis of mitochondria using transmission electron microscopy. Representative images of mitochondria identified in thin-sectioned specimens of LLC-PK_1 cells stably expressing mito-GFP (**a**) or FB-GFP fusion protein (**b-f**) are shown. Bars, 0.25 μm

et al. 2004; Paumard et al. 2002; Velours et al. 2009). These data strongly imply that ATP synthase dimers and oligomers, formation of which requires subunits *e* or *g*, are actively engaged in generating cristae morphology (Arselin et al. 2004; Paumard et al. 2002; Velours et al. 2009). Single-particle analyses of isolated ATP synthase dimers, as well as cryo-electron tomography of whole mitochondria, provided additional support for the role of dimers and higher oligomeric species of ATP synthase in generating the inner membrane curvature (Dudkina et al. 2005; Minauro-Sanmiguel et al. 2005; Strauss et al. 2008; Thomas et al. 2008).

Mitochondria in LLC-PK$_1$ cells stably expressing FB-GFP fusion protein display cristae that either form half-rings or localize along the organelle's perimeter (Fig. 3b-f). A notable feature of the cristae is the apparent increase in their thickness. This may result from an increased packing density of membrane proteins within the lipid bilayer. Membrane protein crowding can promote protein-protein interactions by favoring the association reactions, and in the context of the inner mitochondrial membrane, could augment the formation of supramolecular complexes such as the ATP synthasome (Chen et al. 2004) and respirasome (Schagger and Pfeiffer 2000). Thus, structural changes in cristae membranes could enhance the rate of exchange of ATP synthasome substrates across the inner membrane, and/or the rate of substrate channeling within the respirasome (Ko et al. 2003; Wittig and Schagger 2009). In agreement with such a scenario, our preliminary data demonstrate that respiratory control ratio is about two-fold higher in LLC-PK$_1$ cells expressing factor B-GFP than in LLC-PK$_1$ cells expressing mitochondria-targeted GFP, indicating increased coupling of respiration and ATP synthesis in the mitochondria of the former cells.

Mitochondria seen in the upper part of Fig. 1c exhibit morphology reminiscent of the "beads on a string" morphology described in studies of HeLa cells depleted of the inner mitochondrial membrane protein OPA1 using siRNA (Griparic et al. 2004). However, inspection of electron micrographs presented in their study, as well as data from a subsequent study on the OPA1 counterpart in *C. elegans* (Kanazawa et al. 2008), suggests that, at the ultrastructural level, the effects of OPA1 depletion and factor B over-expression on cristae morphology are distinct. Of particular interest, however, is the possible role for the yeast OPA1 homolog in controlling the stability of the yeast ATP synthase subunit *e* (Amutha et al. 2004).

Electron tomographic reconstructions of animal mitochondria have revealed the dynamic nature of the inner mitochondrial membrane, suggesting that the processes of fission and fusion actively contribute to maintaining the tubular-lamellar balance of the inner membrane (Mannella 2008). The palm of a human hand, with the fingers either kept apart or together, could provide a crude, yet vivid, analogy of the structural transitions that may occur at the level of an individual crista. Here we demonstrate for the first time that coupling factor B participates in regulating the morphology of mitochondria and that its over-expression apparently displaces the tubular-lamellar balance of the inner membrane toward the tubular form. The molecular mechanisms underlying this remodeling of the inner membrane, and its bioenergetic consequences, remain to be elucidated.

Acknowledgements I thank Dr. George Sachs for access to a laser scanning confocal microscope LSM 510, Dr. Olga Vagin for advice on confocal microscopy, Marianne Cilluffo for preparing specimens and for help with transmission electron microscopy, and Dr. William C. Claycomb for providing the HL-1 cells. This work was supported by NIH grant R01GM066085. I dedicate this article to Dr. Youssef Hatefi on the occasion of his 80th birthday.

References

Amutha B, Gordon DM, Gu Y, Pain D (2004) Biochem J 381:19–23
Arselin G, Vaillier J, Salin B, Schaeffer J, Giraud MF, Dautant A, Brèthes D, Velours J (2004) J Biol Chem 279:40392–40399
Belogrudov GI (2002) Arch Biochem Biophys 406:271–274
Belogrudov GI (2006) Arch Biochem Biophys 451:68–78
Belogrudov GI (2007) Arch Biochem Biophys 461:95–103
Belogrudov GI (2008) Arch Biochem Biophys 473:76–87
Belogrudov GI (2009) J Bioenerg Biomembr 41:137–143
Belogrudov GI, Hatefi Y (2002) J Biol Chem 277:6097–6103
Belogrudov GI, Tomich JM, Hatefi Y (1995) J Biol Chem 270:2053–2060
Belogrudov GI, Tomich JM, Hatefi Y (1996) J Biol Chem 271:20340–20345
Benard G, Rossignol R (2008) Antioxid Redox Signal 10:1313–1342
Beraud N, Pelloux S, Usson Y, Kuznetsov AV, Ronot X, Tourneur Y, Saks V (2009) J Bioenerg Biomembr 41:195–214
Berman SB, Chen YB, McCaffery JM, Rucker EB 3 rd, Goebbels S, Nave KA, Arnold BA, Jonas EA, Pineda FJ, Hardwick JM (2009) J Cell Biol 184:707–719
Chan DC (2006) Annu Rev Cell Dev 22:79–99
Chen C, Ko Y, Delannoy M, Ludtke SJ, Chiu W, Pedersen PL (2004) J Biol Chem 279:31761–31768
Collins TJ, Berridge MJ, Lipp P, Bootman MD (2002) EMBO J 21:1616–1627
de Brito OM, Scorrano L (2008) Nature 456:605–610
Dudkina NV, Heinemeyer J, Keegstra W, Boekema EJ, Braun HP (2005) FEBS Lett 579:5769–5772
Fillingame RH, Angevine CM, Dmitriev OY (2003) FEBS Lett 555:29–34
Griparic L, van der Wel NN, Orozco IJ, Peters PJ, van der Bliek AM (2004) J Biol Chem 279:18792–18798
Hatefi Y (1985) Annu Rev Biochem 54:1015–1069
Hong S, Pedersen PL (2008) Microbiol Mol Biol Rev 72:590–641
Junge W, Sielaff H, Engelbrecht S (2009) Nature 459:364–370
Kanazawa T, Zappaterra MD, Hasegawa A, Wright AP, Newman-Smith ED, Buttle KF, McDonald K, Mannella CA, van der Bliek AM (2008) PloS Genet 4:e1000022
Ko YH, Delannoy M, Hullihen J, Chiu W, Pedersen PL (2003) J Biol Chem 278:12305–12309

Kopecky J, Glaser E, Norling B, Ernster L (1981) FEBS Lett 131:208–212
Lam KW, Warshaw JB, Sanadi DR (1967) Arch Biochem Biophys 119:477–484
Lee JK, Belogrudov GI, Stroud RM (2008) Proc Natl Acad Sci USA 105:13379–13384
Lee CP, Ernster L (1965) Biochem Biophys Res Commun 18:523–529
Mannella CA (2008) Ann N Y Acad Sci 1147:171–179
Minauro-Sanmiguel F, Wilkens S, Garcia JJ (2005) Proc Natl Acad Sci USA 102:12356–12357
Pauleau AL, Galuzzi L, Scholz SR, Larochette N, Kepp O, Kroemer G (2008) Cell Death Differ 15:616–618
Paumard P, Vaillier J, Coulary B, Schaeffer J, Soubannier V, Mueller DM, Brèthes D, di Rago JP, Velours J (2002) EMBO J 21:221–230
Sanadi DR (1982) Biochim Biophys Acta 683:39–56
Schagger H, Pfeiffer K (2000) EMBO J 19:1777–1783
Stephenson G, Sanadi DR (1989) Biochem Int 19:1087–1094
Strauss M, Hofhaus G, Schroder RR, Kuhlbrandt W (2008) EMBO J 27:1154–1160
Thomas D, Bron P, Weinmann T, Dautant A, Giraud MF, Paumard P, Salin B, Cavalier A, Velours J, Brèthes D (2008) Biol Cell 100:591–601
Velours J, Dautant A, Salin B, Sagot I, Brethes D (2009) Int J Biochem Cell Biol 41:1783–1789
Vik SB, Long JC, Wada T, Zhang D (2000) Biochim Biophys Acta 1458:457–466
Wasilewski M, Scorrano L (2009) Trends Endocrinol Metab 20:287–294
Wittig I, Schagger H (2009) Biochim Biophys Acta 1787:672–680